Control of Ferromagnetic Relaxation in Magnetic Thin Films through Thermally Induced Interfacial Spin Transfer

Lei Lu, Yiyan Sun, Michael Jantz, and Mingzhong Wu

Phys. Rev. Lett. **108**, 257202 — Published 19 June 2012

DOI: 10.1103/PhysRevLett.108.257202

Control of Ferromagnetic Relaxation in Magnetic Thin Films through Thermally Induced Interfacial Spin Transfers

Lei Lu, Yiyan Sun, Michael Jantz, and Mingzhong Wu*

Department of Physics, Colorado State University, Fort Collins, Colorado 80523, USA

Relaxation control in magnetic thin films via thermally induced interfacial spin transfers was demonstrated for the first time. The experiments used a tri-layered structure that consisted of an yttrium iron garnet (YIG) thin film grown on a gadolinium gallium garnet substrate and capped with a nm-thick Pt layer. As a temperature gradient is applied across the thickness of the structure, there exists a spin angular momentum transfer across the YIG/Pt interface. This spin transfer results in a torque on YIG magnetic moments. The torque can either speed up or slow down the relaxation in the YIG film, depending on the sign of the temperature gradient with respect to the tri-layered structure.

Recently, three approaches have been demonstrated that can control ferromagnetic relaxation in magnetic thin films. The first approach makes use of the flow of spin-polarized electrons through the films [1,2]. The second takes the advantage of the injection of spin-polarized electrons into the films [3]. The third uses the scattering of spin-polarized electrons off the film surfaces [4,5]. Although these approaches differ in the way of using spin-polarized electrons, they all rely on angular momentum transfers between the spin-polarized conduction electrons and the spins in the films to realize relaxation control.

This Letter reports on a new approach for relaxation control. Specifically, this letter presents the control of spin-wave resonance linewidth in magnetic thin films through thermally induced interfacial spin transfers. Experiments use a tri-layered structure element that consists of a micron-thick yttrium iron garnet (YIG) film grown on a sub-millimeter-thick gadolinium gallium garnet (GGG) substrate and capped with a nanometer-thick Pt layer. The YIG film is ferrimagnetic, while the GGG substrate and the Pt layer are both paramagnetic. A temperature gradient is established across the thickness of the GGG/YIG/Pt element. This temperature gradient produces, through the spin Seebeck effect, a spin current that flows from the YIG/Pt interface into the Pt layer [6,7,8,9,10,11]. The net effect of the spin current is an angular momentum transfer between the spins in the YIG film and the conduction electrons in the Pt layer. This momentum transfer results in a torque on the magnetic moments in the YIG film. The torque can either speed up or slow down the ferromagnetic relaxation in the YIG film, depending on the direction of the temperature gradient with respect to the tri-layered structure. This control of the relaxation manifests itself as changes in the linewidths of lateral spin-wave resonance modes in the YIG film.

Two points should be emphasized. (1) There exists a substantial difference between the approach demonstrated below and those demonstrated previously [1-5]. Previous approaches all rely on external systems to supply spin-polarized electrons. In contrast, the new approach has no need of an external supply of spin-polarized electrons, but requires the application of a temperature gradient. (2) The new approach is simple yet very efficient. As demonstrated below, an easily accessible temperature gradient can produce a change in damping that is larger than the intrinsic damping in YIG materials.

Figure 1 shows the experimental configuration. The core component is a GGG/YIG/Pt rectangular element. A temperature gradient is applied across the thickness of the GGG/YIG/Pt element by placing it against two Peltier devices, which are not shown in Fig. 1. An external field H is applied in the $+y$ direction to magnetize the YIG film. A microwave field h is applied along the x axis to excite spin waves in the YIG film. Due to the confinement of

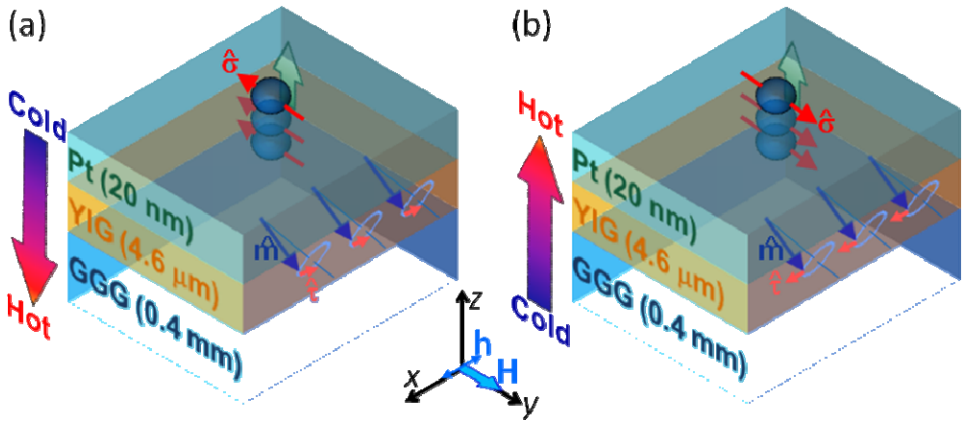

FIG. 1. Experimental configuration. Graphs (a) and (b) show the situations for two difference temperature gradients.

YIG lateral dimensions, the spin waves are standing modes with wavenumbers $k = \sqrt{(m\pi/a)^2 + (n\pi/b)^2}$, where a and b are the dimensions of the YIG film along the x and y axes, respectively, and m and n denote the mode indexes.

The relaxation control can be interpreted as follows. (1) The temperature gradient results in a difference between the distributions of the magnon temperature T_m and the phonon temperature T_p across the YIG film thickness [12]. (2) The difference between T_m and T_p at the YIG/Pt interface gives rise to a spin current in the Pt layer. In the Pt layer in Fig. 1, the small spheres represent polarized electrons, the horizontal arrows through the spheres show the magnetic moment directions ($\hat{\boldsymbol{\sigma}}$) of the electrons, and the vertical arrows indicate the directions of the spin currents. (3) The net effect of (2) is an angular momentum transfer between the localized electrons in the YIG film and the conduction electrons in the Pt layer. This transfer is realized through the *s*-*d* exchange interactions at the YIG/Pt interface [13]. (4) The angular momentum transfer then produces a torque on the magnetic moments at the YIG surface and thereby affects the relaxation of those moments. (5) The effect of this spin transfer torque (STT) is extended to other moments across the YIG film thickness via dipolar and exchange interactions. In the YIG layer in Fig. 1, the longer arrows indicate magnetic moment directions ($\hat{\mathbf{m}}$), and the shorter arrows indicate STT directions ($\hat{\boldsymbol{\tau}}$).

Two points should be made about the above interpretation. First, the difference between the distributions of T_m and T_p across the YIG film thickness originates from the fact that the magnon-magnon relaxation process is much faster than the magnon-phonon relaxation process. In YIG materials, the magnon-magnon relaxation time is in the 10^{-9} – 10^{-7} s range, while the magnon-phonon relaxation time is on the order of 10^{-6} s [12]. Due to the fast magnon-magnon relaxation, T_m is relatively constant across the YIG film thickness and its distribution deviates from that of

T_p [10,12]. Note that the variation of T_p is determined by the temperature gradient applied.

Second, the generation of a spin current in the Pt layer derives from the fact that, at a finite temperature, there coexist (1) a spin pumping-induced spin current $\mathbf{I}_{sp}$ flowing from the interface into the Pt layer and (2) a fluctuating spin current $\mathbf{I}_{fl}$ flowing from the Pt layer towards the interface [12]. Note that the "spin pumping" involved here is thermally activated and does not refer to the conventional spin pumping which is due to the application of external microwaves [14]. The magnitude of $\mathbf{I}_{sp}$ depends on T_m in the YIG layer near the interface, while that of $\mathbf{I}_{fl}$ depends on T_p in the Pt layer. Note that T_p in the Pt layer is essentially the same as T_p in the YIG layer near the interface since the Pt layer is very thin in comparison with the YIG film. The net spin current in the Pt layer is [12]

$$\langle \mathbf{I} \rangle_y = \langle \mathbf{I}_{sp} \rangle_y + \langle \mathbf{I}_{fl} \rangle_y = \frac{2|\gamma| \hbar g_r k_B}{4\pi M_s V} (T_m - T_p) \tag{1}$$

where $|\gamma|$ is the gyromagnetic ratio, g_r is the real part of the spin mixing conductance at the YIG/Pt interface, $4\pi M_s$ is the YIG saturation induction, and V is the YIG volume in which the spins are involved in the interfacial spin transfer. One can see from Eq. (1) that a difference between T_m and T_p results in a nonzero spin current in the Pt layer.

For the configuration in Fig. 1(a), the temperature gradient results in $T_m > T_p$ at the YIG/Pt interface and $I_y > 0$ in the Pt layer. This configuration is similar to the conventional spin pumping effect [14] for which the spin current consists of polarized electrons with magnetic moments anti-parallel to the precession axis of the YIG magnetic moments, namely, $\hat{\boldsymbol{\sigma}} // \langle -\hat{\mathbf{m}} \rangle$. The net effect of this current is a torque on the YIG moments that enhances the relaxation. When the temperature gradient is reversed, as shown in Fig. 1(b), one can expect $T_m < T_p$ at the interface and a spin current with $I_y < 0$ and $\hat{\boldsymbol{\sigma}} // \langle \hat{\mathbf{m}} \rangle$ in the Pt layer. In this case, the torque counters the relaxation and thereby plays a role of a negative damping. It is important to emphasize that the asymmetry of the GGG/YIG/Pt structure is critical for the realization of the relaxation control. For a symmetric structure such as Pt/YIG/Pt, one might have opposite effects at the two YIG/Pt interfaces and an overall change of zero in the relaxation rate.

For the data presented below, the sample was prepared with three steps: (1) the growth of a 4.6-μm-thick YIG film on a 0.4-mm-thick GGG substrate by liquid phase epitaxy, (2) the growth of a 20-nm-thick Pt layer on the YIG film by pulsed laser deposition, and (3) the cutting of the GGG/YIG/Pt structure into a rectangular element with a=2.0 mm and b=2.2 mm. The temperatures of the two surfaces of the element were monitored by two

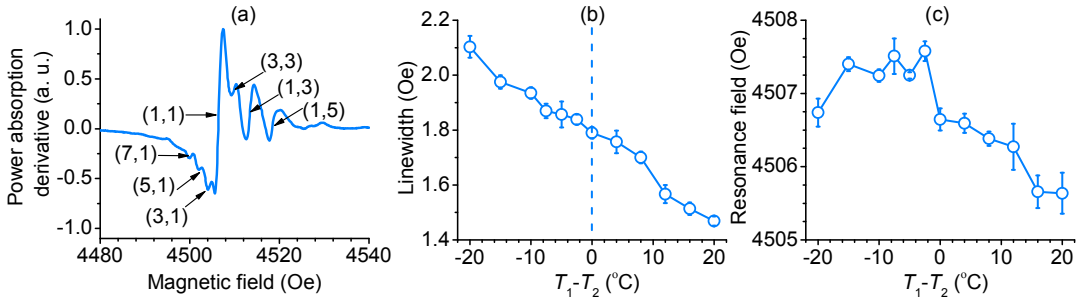

FIG. 2. (a) Spin-wave resonance profile of a GGG/YIG/Pt element measured at T_1=T_2=30 °C. (b) Linewidth and (c) resonance field of mode (1,1) as a function of T_1-T_2. T_1 and T_2 denote the temperatures of the top (Pt) and bottom (GGG) surfaces, respectively. In (a), the integers indicate the indexes of resonance modes. The data in (b) and (c) were obtained with T_1 fixed at 30 °C and T_2 varied from 10 °C to 50 °C.

thermocouples. In the discussions below, the temperatures at the top (Pt) and bottom (GGG) surfaces are referred to as T_1 and T_2, respectively. The spin-wave resonance measurements were carried out at 15 GHz in a shorted waveguide. Measurements were also carried out on a control sample GGG(0.4mm)/YIG(4.6μm)/Cu(20nm) that had a=3.0 mm and b=2.2 mm. Two notes should be made about the data presented below. (1) All the linewidth data are peak-to-peak linewidths. (2) For the data points with error bars, the points show averaged values over 6 measurements and the bars give the corresponding standard deviations.

Figure 2 shows representative results for the GGG/YIG/Pt sample. Graph (a) shows a spin-wave resonance profile measured at T_1=T_2=30 °C. The integers show mode indexes (m, n) obtained on the basis of the spin-wave theory [15] and the resonance fields. Graphs (b) and (c) show the linewidth and resonance field of mode (1,1), respectively, as a function of T_1-T_2. They were obtained with T_1 fixed at 30 °C and T_2 varied from 10 °C to 50 °C.

The data in Fig. 2 show three results. (1) There exist a number of spin-wave resonance modes in the YIG film. In (a), the modes to the left and right of mode (1,1) are usually classified as surface and backward volume modes, respectively [15,16]. (2) The linewidth of mode (1,1) changes significantly with the temperature gradient. When the top surface is hot, the linewidth decreases with an increase in $|T_1 - T_2|$; when the top surface is cold, the linewidth increases with $|T_1 - T_2|$. These responses agree with the expectations. (3) The overall changes in linewidth and resonance field are ±17.8% and ±0.02%, respectively. These values indicate that the heating-associated resonance shift is insignificant and the observed change in linewidth is not due to a usual heating effect.

Figure 3 shows the data for other modes. In each panel, the top graph shows the linewidth vs. T_1-T_2 response, and the bottom graph shows the resonance field as a function of T_1-T_2. The percentages in each graph give the range of the overall linewidth or field change. Two important results are evident in Fig. 3. First, except the top graph in

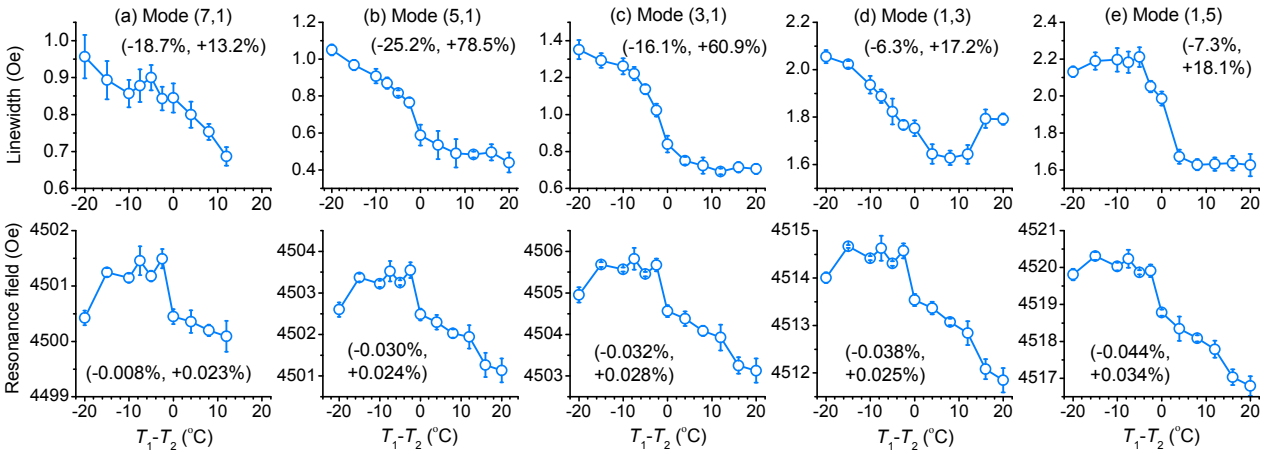

FIG. 3. Linewidth (top) and resonance field (bottom) as a function of T_1-T_2 for different spin-wave resonance modes, as indicated. All the data were measured with T_1 kept constant at 30 °C and T_2 varied from 10 °C to 50 °C.

(d), all the graphs show responses similar to those of mode (1,1). Second, the surface modes show stronger STT effects than the backward volume modes. This agrees with the recent observation for spin pumping in YIG/Pt structures that surface modes showed significantly higher spin-pumping efficiencies than backward volume modes [17]. This behavior results from the difference in spin-wave amplitude distributions across the YIG film thickness for different modes [15,16]. Specifically, the amplitude for a surface spin wave is strong on one of the film surfaces and decays exponentially as one moves from the film surface into the film volume. In contrast, a backward volume mode has uniform amplitude across the film thickness. For the same microwave power applied, the surface modes have larger amplitudes near the YIG/Pt interface than the backward volume modes, and the net result is a larger spin transfer at the YIG/Pt interface and a larger change in linewidth. This is essentially the same as in conventional spin pumping in which the magnitude of the spin current increases with the angle of the magnetization precession.

The data in Figs. 2 and 3 together demonstrate the feasibility of resonance linewidth control through thermally induced spin transfers. For such control, both the temperature gradient and the Pt layer play crucial roles: the former gives rise to a spin current and the latter acts as a sink to dissipate the spin current. Such roles were clearly demonstrated by additional measurements with different configurations and different samples.

Figure 4 shows data for the GGG/YIG/Cu sample. One can see that, with a change in T_1-T_2, the resonance field changes in the same manner as the GGG/YIG/Pt sample does, while the linewidth exhibits no notable changes. These responses result from the fact that the Cu layer cannot act as a spin sink because Cu has a long electron mean free path λ_f, a long spin-flip length λ_{sf}, and weak spin-orbit coupling. The spin diffusion length in Cu is $l_{sd} = \sqrt{(1/3)\lambda_f \lambda_{sf}} \approx 500$ nm [18]. This length is significantly larger than the thickness of the Cu layer in the

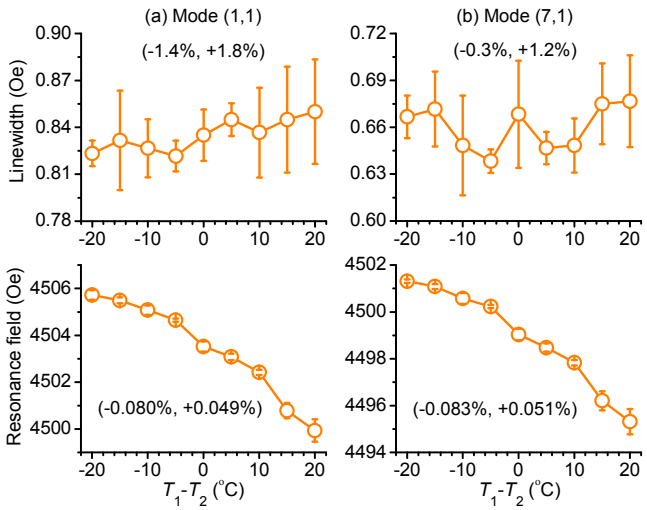

FIG. 4. Linewidth (top) and resonance field (bottom) as a function of T_1-T_2 for two different modes. The data were measured for a GGG/YIG/Cu sample with T_1=30 °C and T_2=10~50 °C.

GGG/YIG/Cu sample. In contrast, the spin diffusion length in Pt is only about 10 nm [19], which is smaller than the thickness of the Pt layer in the GGG/YIG/Pt sample.

Figure 5 shows data for the GGG/YIG/Pt sample measured with T_1=T_2. The data show two results. (1) The resonance field increases significantly with the sample temperature, with an overall change of larger than 0.6%. This response originates from the fact that $4\pi M_s$ decreases with temperature. (2) Although the field changes are one order of magnitude larger than the changes shown in Figs. 2 and 3, the changes in linewidth are smaller than those shown in Figs. 2 and 3. Similar results were obtained for the GGG/YIG/Cu sample. These results clearly demonstrate that the linewidth changes in Figs. 2 and 3 do not result from the heating or cooling of the YIG film. Rather, it results from the temperature gradient.

One can use the measured linewidth changes to estimate the STT-produced changes in damping, $\Delta\alpha_{STT}$, if one assumes that (1) the STT-produced damping is Gilbert-like and (2) the spin-wave linewidth is close to the linewidth of a uniform mode. Figure 6 shows the $\Delta\alpha_{STT}$ values estimated with the data in Fig. 2(b). One can see that a temperature gradient of 20 °C gives rise to a change in damping of about 5.1×10^{-5}. The largest linewidth change

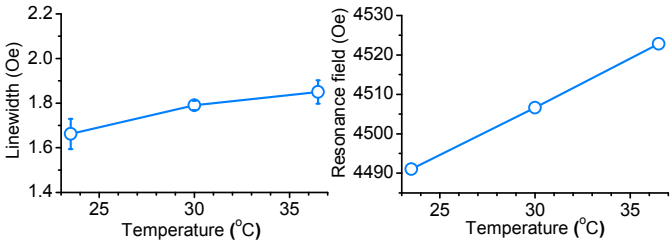

FIG. 5. Linewidth and resonance field of mode (1,1) as a function of the sample temperature for the GGG/YIG/Pt sample.

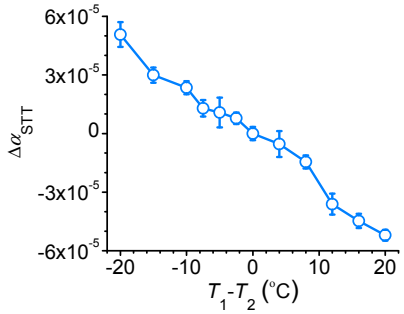

FIG. 6. STT-produced change in damping constant α as a function of T_1- T_2. The $\Delta\alpha_{STT}$ values were obtained from the data shown in Fig. 2(b).

was observed for mode (3,1). This change corresponds to a $\Delta\alpha_{STT}$ value of about 8.3×10^{-5}. These changes are substantial as they are larger than the intrinsic damping in YIG materials, which is $\alpha_0 = 3\times10^{-5}$. Note that all the measurements in this work were carried out with magnetic fields applied in the film planes. Future work on the determination of $\Delta\alpha_{STT}$ through measurements with out-of-plane fields at different frequencies is of high interest.

Two points should be emphasized. (1) It is the overall temperature gradient across the GGG/YIG/Pt structure, rather than the gradient across the YIG film, that is responsible for the demonstrated effects. This is because the phonons have long propagation length and the magnons in the YIG film can feel the temperature in the GGG substrate [20]. (2) Although the demonstrations made use of YIG-based structures, one can expect similar effects in structures consisted of ferromagnetic metallic films. Also, it should be mentioned that the growth of a Pt layer on a YIG film does lead to a certain increase in the damping of the YIG film. Future work on the study of physical mechanisms for this increase and possible methods for avoiding it is of great interest.

In conclusion, this work demonstrated the control of linewidths of spin-wave resonance modes in a GGG/YIG/Pt structure through the application of a temperature gradient across the structure thickness. Such control relies on the thermally induced spin angular momentum transfers across the YIG/Pt interface. The results not only demonstrate a new approach for relaxation control, but also suggest a new mechanism for spin torque oscillators, in which the spin torque results from thermally induced angular momentum transfer.

This work was supported in part by the U. S. National Science Foundation (DMR-0906489), the U. S. Army Research Office (W911NF-11-C-0075), and the U. S. National Institute of Standards and Technology (60NANB10D011).

*Corresponding author. E-mail: mwu@lamar.colostate.edu

[1]G. D. Fuchs, J. C. Sankey, V. S. Pribiag, L. Qian, P. M. Braganca, A. G. F. Garcia, E. M. Ryan, Z. P. Li, O. Ozatay, D. C. Ralph, and R. A. Buhrman, Appl. Phys. Lett. **91**, 062507 (2007) .

[2]D. C. Ralph and M. D. Stiles, J. Magn. Magn. Mater. **320**, 1190 (2008).

[3]K. Ando, S. Takahashi, K. Harii, K. Sasage, J. Ieda, S. Maekawa, and E. Saitoh, Phys. Rev. Lett. **101**, 036601 (2008).

[4] Z. Wang, Y. Sun, M. Wu, V. Tiberkevich, and A, Slavin, Phys. Rev. Lett. **107**, 146602 (2011).

[5] Z. Wang, Y. Sun, Y. Song, M. Wu, H. Schultheiβ, J. E. Pearson, and A. Hoffmann, Appl. Phys. Lett. **99**, 162511 (2011).

[6] K. Uchida, S. Takahashi, K. Harii, J. Ieda, W. Koshibae, K. Ando, S. Maekawa, and E. Saitoh, Nature **455**, 778 (2008).

[7] K. Uchida, J. Xiao, H. Adachi, J. Ohe, S. Takahashi, J. Leda, T. Ota, Y. Kajiwara, H. Umezawa, H. Kawai, G. E. W. Bauer, S. Maekawa, and E. Saitoh, Nature Materials **9**, 894 (2010).

[8] C. M. Jaworski, J. Yang, S. Mack, D. D. Awschalom, J. P. Heremans, and R. C. Myers, Nature Mater. **9**, 898 (2010).

[9] K. Uchida, T. Ota, K. Harii, S. Takahashi, S. Maekawa, Y. Fujikawa, and E. Saitoh, Solid State Commun. **150**, 524 (2010).

[10]C. M. Jaworski, J. Yang, S. Mack, D. D. Awschalom, R. C. Myers, and J. P. Heremans, Phys. Rev. Lett. **106**, 186601 (2011).

[11] E. Padrón-Hernández, A. Azevedo, and S. M. Rezende, Phys. Rev. Lett. 107, 197203 (2011).

[12] J. Xiao, G. E. W. Bauer, K. Uchida, E. Saitoh, and S. Maekawa, Phys. Rev. B **81**, 214418 (2010).

[13] S. Takahashi, E. Saitoh, and S. Maekawa, J. Phys. Conf. Ser. **200**, 062030 (2009).

[14] B. Heinrich and J. A. C. Bland, Ultrathin Magnetic Structures: Fundamentals of Nanomagnetism (Springer, Berlin, 2005).

[15] R. W. Damon and J. R. Eshbach, J. Phys. Chem. Solids **19**, 308 (1961).

[16] D. D. Stancil and A. Prabhakar, *Spin Waves: Theory and Applications* (Springer, New York, 2009).

[17] C. Sandweg, Y. Kajiwara, K. Ando, E. Saitoh, and B, Hillebrands, Appl. Phys. Lett. **97**, 252504 (2010).

[18] T. Kimura, J. Hamrle, and Y. Otani, Phys. Rev. B **72**, 014461 (2005).

[19] L. Vila, T. Kimura, and Y. Otani, Phys. Rev. Lett. **99**, 226604 (2007).

[20] K. Uchida, H. Adachi, T. An, T. Ota, M. Toda, B. Hillebrands, S. Maekawa and E. Saitoh, Nature Materials **10**, 737 (2011).